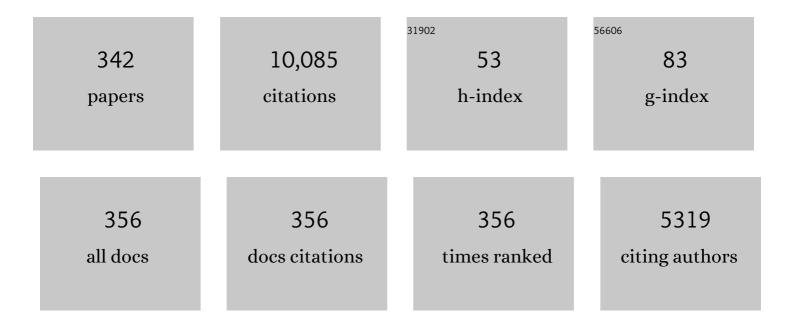
List of Publications by Year in descending order

Source: https://exaly.com/author-pdf/1195277/publications.pdf Version: 2024-02-01



#	Article	IF	CITATIONS
1	Over 1 A/mm drain current density and 3.6ÂW/mm output power density in 2DHG diamond MOSFETs with highly doped regrown source/drain. Carbon, 2022, 188, 220-228.	5.4	10
2	580 V Breakdown Voltage in Vertical Diamond Trench MOSFETs With a P ^{â^'} -Drift Layer. IEEE Electron Device Letters, 2022, 43, 88-91.	2.2	5
3	MOSFETs on (110) Câ \in "H Diamond: ALD Alâ,,Oâ, <i>f</i> /Diamond Interface Analysis and High Performance Normally-OFF Operation Realization. IEEE Transactions on Electron Devices, 2022, 69, 949-955.	1.6	23
4	â~'10 V Threshold Voltage High-Performance Normally-OFF C–Si Diamond MOSFET Formed by p ⁺ -Diamond-First and Silicon Molecular Beam Deposition Approaches. IEEE Transactions on Electron Devices, 2022, 69, 2236-2242.	1.6	11
5	â~'400 mA mm ^{â~'1} Drain Current Density Normally-Off Polycrystalline Diamond MOSFETs. IEEE Electron Device Letters, 2022, 43, 789-792.	2.2	4
6	pH Measurement at Elevated Temperature with Vessel Gate and Oxygen-Terminated Diamond Solution Gate Field Effect Transistors. Sensors, 2022, 22, 1807.	2.1	1
7	An enhanced two-dimensional hole gas (2DHG) C–H diamond with positive surface charge model for advanced normally-off MOSFET devices. Scientific Reports, 2022, 12, 4203.	1.6	7
8	Fluorine-Terminated Polycrystalline Diamond Solution-Gate Field-Effect Transistor Sensor with Smaller Amount of Unexpectedly Generated Fluorocarbon Film Fabricated by Fluorine Gas Treatment. Materials, 2022, 15, 2966.	1.3	0
9	C-Si interface on SiO2/(1 1 1) diamond p-MOSFETs with high mobility and excellent normally-off operation. Applied Surface Science, 2022, 593, 153368.	3.1	11
10	High Temperature Performance of Enhanced Endurance Hydrogen Terminated Transparent Polycrystalline Diamond FET. IEEE Electron Device Letters, 2022, 43, 1101-1104.	2.2	3
11	Electrical Characterization of Metal/Alâ,,Oâ,ƒ/SiOâ,,/Oxidized-Si-Terminated (C–Si–O) Diamond Capacitors. IEEE Transactions on Electron Devices, 2022, 69, 3604-3610.	1.6	5
12	Normally-Off Oxidized Si-Terminated (111) Diamond MOSFETs via ALD-Al ₂ O ₃ Gate Insulator With Drain Current Density Over 300 mA/mm. IEEE Transactions on Electron Devices, 2022, 69, 4144-4152.	1.6	5
13	300 mA/mm Drain Current Density P-Type Enhancement-Mode Oxidized Si-terminated (111) Diamond MOSFETs with ALD Al ₂ 0 ₃ Gate Insulator. , 2022, , .		0
14	Over 59 mV pH â~'1 Sensitivity with Fluorocarbon Thin Film via Fluorine Termination for pH Sensing Usin Boronâ€Doped Diamond Solutionâ€Gate Fieldâ€Effect Transistors. Physica Status Solidi (A) Applications and Materials Science, 2021, 218, 2000278.	g 0.8	3
15	Microwave diamond devices technology: Fieldâ€effect transistors and modeling. International Journal of Numerical Modelling: Electronic Networks, Devices and Fields, 2021, 34, .	1.2	9
16	Drain Current Density Over 1.1 A/mm in 2D Hole Gas Diamond MOSFETs With Regrown p++-Diamond Ohmic Contacts. IEEE Electron Device Letters, 2021, 42, 204-207.	2.2	26
17	C–Si bonded two-dimensional hole gas diamond MOSFET with normally-off operation and wide temperature range stability. Carbon, 2021, 175, 525-533.	5.4	26
18	Space-charge-controlled field emission analysis of current conduction in amorphous and crystallized atomic-layer-deposited Al2O3 on GaN. Journal of Applied Physics, 2021, 129, .	1.1	6

#	Article	IF	CITATIONS
19	Microstructure, Morphology and Magnetic Property of (001)-Textured MnAlGe Films on Si/SiO ₂ Substrate. Materials Transactions, 2021, 62, 680-687.	0.4	3
20	(111) vertical-type two-dimensional hole gas diamond MOSFETs with hexagonal trench structures. Carbon, 2021, 176, 349-357.	5.4	8
21	Low ON-Resistance (2.5 mΩ · cm ²) Vertical-Type 2-D Hole Gas Diamond MOSFETs With Trench Gate Structure. IEEE Transactions on Electron Devices, 2021, 68, 3490-3496.	1.6	9
22	Crystal analysis of grain boundaries in boron-doped diamond superconducting quantum interference devices operating above liquid helium temperature. Carbon, 2021, 181, 379-388.	5.4	2
23	High Output Power Density of 2DHG Diamond MOSFETs With Thick ALD-Al ₂ O ₃ . IEEE Transactions on Electron Devices, 2021, 68, 3942-3949.	1.6	18
24	Highly aligned 2D NV ensemble fabrication from nitrogen-terminated (111) surface. Carbon, 2021, 180, 127-134.	5.4	4
25	Postdeposition annealing effect on atomic-layer-deposited Al2O3 gate insulator on (001) β-Ga2O3. Journal of Vacuum Science and Technology B:Nanotechnology and Microelectronics, 2021, 39, .	0.6	2
26	Ten Years Progress of Electrical Detection of Heavy Metal Ions (HMIs) Using Various Field-Effect Transistor (FET) Nanosensors: A Review. Biosensors, 2021, 11, 478.	2.3	21
27	Effect of Surface Charge Model in the Characterization of Two-dimensional Hydrogenated Nanocrystalline-diamond Metal Oxide Semiconductor Field Effect Transistor (MOSFET) with Device Simulation. , 2021, , .		0
28	Over 12000 A/cm ² and 3.2 m\$Omega\$ cm ² Miniaturized Vertical-Type Two-Dimensional Hole Gas Diamond MOSFET. IEEE Electron Device Letters, 2020, 41, 111-114.	2.2	21
29	Feasibility Study of TiO _{<i>x</i>} Encapsulation of Diamond Solutionâ€Gate Fieldâ€Effect Transistor Metal Contacts for Miniature Biosensor Applications. Physica Status Solidi (A) Applications and Materials Science, 2020, 217, 2000634.	0.8	0
30	Local initial heteroepitaxial growth of diamond (111) on Ru (0001)/c-sapphire by antenna-edge-type microwave plasma chemical vapor deposition. Applied Physics Letters, 2020, 117, .	1.5	7
31	Epitaxial Combination of Two-Dimensional Hexagonal Boron Nitride with Single-Crystalline Diamond Substrate. ACS Applied Materials & Interfaces, 2020, 12, 46466-46475.	4.0	13
32	Application of 2DHG Diamond p-FET in Cascode With Normally-OFF Operation and a Breakdown Voltage of Over 1.7 kV. IEEE Transactions on Electron Devices, 2020, 67, 4006-4009.	1.6	5
33	Postdeposition annealing effect on the reliability of atomic-layer-deposited Al2O3 films on GaN. Journal of Vacuum Science and Technology B:Nanotechnology and Microelectronics, 2020, 38, .	0.6	6
34	Oxidized Si terminated diamond and its MOSFET operation with SiO2 gate insulator. Applied Physics Letters, 2020, 116, .	1.5	33
35	Dynamic space-charge-controlled field emission model of current conduction in metal–insulator–semiconductor capacitors. Journal of Applied Physics, 2020, 127, .	1.1	5
36	Gate/insulator-interfacial-dipole-controlled current conduction in Al2O3 metal-insulator-semiconductor capacitors. Journal of Applied Physics, 2019, 126, .	1.1	10

#	Article	IF	CITATIONS
37	Correlation between the Carbon Nanotube Growth Rate and Byproducts in Antennaâ€Type Remote Plasma Chemical Vapor Deposition Observed by Vacuum Ultraviolet Absorption Spectroscopy. Small, 2019, 15, e1901504.	5.2	4
38	Electrical property measurement of two-dimensional hole-gas layer on hydrogen-terminated diamond surface in vacuum-gap-gate structure. Applied Physics Letters, 2019, 114, .	1.5	6
39	Pointâ€Arc Remote Plasma Chemical Vapor Deposition for Highâ€Quality Singleâ€Crystal Diamond Selective Growth. Physica Status Solidi (A) Applications and Materials Science, 2019, 216, 1900227.	0.8	3
40	Carbon Nanotube Forests on SiC: Structural and Electrical Properties. , 2019, , 605-620.		0
41	Single-crystalline boron-doped diamond superconducting quantum interference devices with regrowth-induced step edge structure. Scientific Reports, 2019, 9, 15214.	1.6	7
42	Nitrogen-Terminated Diamond Surface for Nanoscale NMR by Shallow Nitrogen-Vacancy Centers. Journal of Physical Chemistry C, 2019, 123, 3594-3604.	1.5	46
43	Deoxyribonucleic-acid-sensitive Polycrystalline Diamond Solution-gate Field-effect Transistor with a Carboxyl-terminated Boron-doped Channel. Analytical Sciences, 2019, 35, 923-927.	0.8	3
44	Triple nitrogen-vacancy centre fabrication by C5N4Hn ion implantation. Nature Communications, 2019, 10, 2664.	5.8	33
45	Normally-OFF Two-Dimensional Hole Gas Diamond MOSFETs Through Nitrogen-Ion Implantation. IEEE Electron Device Letters, 2019, 40, 933-936.	2.2	31
46	Advanced photo-assisted capacitance–voltage characterization of insulator/wide-bandgap semiconductor interface using super-bandgap illumination. Journal of Applied Physics, 2019, 125, .	1.1	9
47	Carbon 1s X-ray photoelectron spectra of realistic samples of hydrogen-terminated and oxygen-terminated CVD diamond (111) and (001). Diamond and Related Materials, 2019, 93, 105-130.	1.8	25
48	3.8 W/mm RF Power Density for ALD Al ₂ O ₃ -Based Two-Dimensional Hole Gas Diamond MOSFET Operating at Saturation Velocity. IEEE Electron Device Letters, 2019, 40, 279-282.	2.2	83
49	Carboxyl-functionalized graphene SGFET: pH sensing mechanism and reliability of anodization. Diamond and Related Materials, 2019, 91, 15-21.	1.8	10
50	Time-dependent dielectric breakdown of atomic-layer-deposited Al2O3 films on GaN. Journal of Applied Physics, 2018, 123, .	1.1	19
51	In-plane electrical conduction mechanisms of highly dense carbon nanotube forests on silicon carbide. Journal of Applied Physics, 2018, 123, 045104.	1.1	3
52	Heteroepitaxial Diamond Field-Effect Transistor for High Voltage Applications. IEEE Electron Device Letters, 2018, 39, 51-54.	2.2	17
53	Role of Carboxyl and Amine Termination on a Boron-Doped Diamond Solution Gate Field Effect Transistor (SGFET) for pH Sensing. Sensors, 2018, 18, 2178.	2.1	13
54	Ionic-liquid-gating setup for stable measurements and reduced electronic inhomogeneity at low temperatures. Review of Scientific Instruments, 2018, 89, 103903.	0.6	2

#	Article	IF	CITATIONS
55	Irradiation-Induced Modification of the Superconducting Properties of Heavily-Boron-Doped Diamond. Physical Review Applied, 2018, 10, .	1.5	7
56	Superconductivity in nano- and micro-patterned high quality single crystalline boron-doped diamond films. Diamond and Related Materials, 2018, 90, 181-187.	1.8	9
57	Vertical-type two-dimensional hole gas diamond metal oxide semiconductor field-effect transistors. Scientific Reports, 2018, 8, 10660.	1.6	40
58	Electrical contact properties between carbon nanotube ends and a conductive atomic force microscope tip. Journal of Applied Physics, 2018, 123, .	1.1	4
59	Lithographically engineered shallow nitrogen-vacancy centers in diamond for external nuclear spin sensing. New Journal of Physics, 2018, 20, 083029.	1.2	18
60	Post-deposition-annealing effect on current conduction in Al2O3 films formed by atomic layer deposition with H2O oxidant. Journal of Applied Physics, 2017, 121, .	1.1	16
61	Normally-Off C–H Diamond MOSFETs With Partial C–O Channel Achieving 2-kV Breakdown Voltage. IEEE Electron Device Letters, 2017, 38, 363-366.	2.2	144
62	Smart Power Devices and ICs Using GaAs and Wide and Extreme Bandgap Semiconductors. IEEE Transactions on Electron Devices, 2017, 64, 856-873.	1.6	106
63	Aptamer strategy for ATP detection on nanocrystalline diamond functionalized by a nitrogen and hydrogen radical beam system. Journal of Applied Physics, 2017, 121, .	1.1	6
64	Vertical edge graphite layer on recovered diamond (001) after highâ€dose ion implantation and highâ€ŧemperature annealing. Physica Status Solidi (B): Basic Research, 2017, 254, 1700040.	0.7	4
65	Durability-enhanced two-dimensional hole gas of C-H diamond surface for complementary power inverter applications. Scientific Reports, 2017, 7, 42368.	1.6	85
66	High Voltage Stress Induced in Transparent Polycrystalline Diamond Field-Effect Transistor and Enhanced Endurance Using Thick Al ₂ O ₃ Passivation Layer. IEEE Electron Device Letters, 2017, 38, 607-610.	2.2	23
67	Sheet resistance underneath the Au ohmic-electrode on hydrogen-terminated surface-conductive diamond (001). Diamond and Related Materials, 2017, 80, 93-98.	1.8	7
68	Vertical edge graphite layer on recovered diamond (001) after high-dose ion implantation and high-temperature annealing (Phys. Status Solidi B 9/2017). Physica Status Solidi (B): Basic Research, 2017, 254, 1770249.	0.7	0
69	Fabrication of photo-electrochemical biosensors for ultrasensitive screening of mono-bioactive molecules: the effect of geometrical structures and crystal surfaces. Journal of Materials Chemistry B, 2017, 5, 7985-7996.	2.9	88
70	Effect of a radical exposure nitridation surface on the charge stability of shallow nitrogen-vacancy centers in diamond. Applied Physics Express, 2017, 10, 055503.	1.1	19
71	Charge state stabilization of shallow nitrogen vacancy centers in diamond by oxygen surface modification. Japanese Journal of Applied Physics, 2017, 56, 04CK08.	0.8	46
72	Threshold voltage control of electrolyte solution gate field-effect transistor by electrochemical oxidation. Applied Physics Letters, 2017, 111, .	1.5	7

#	Article	IF	CITATIONS
73	Polycrystalline Boron-doped Diamond Electrolyte-solution-gate Field-effect Transistor Applied to the Measurement of Water Percentage in Ethanol. Analytical Sciences, 2017, 33, 1193-1196.	0.8	4
74	An All-Solid-State pH Sensor Employing Fluorine-Terminated Polycrystalline Boron-Doped Diamond as a pH-Insensitive Solution-Gate Field-Effect Transistor. Sensors, 2017, 17, 1040.	2.1	7
75	Aptamer-Based Carboxyl-Terminated Nanocrystalline Diamond Sensing Arrays for Adenosine Triphosphate Detection. Sensors, 2017, 17, 1686.	2.1	4
76	Space-charge-controlled field emission model of current conduction through Al2O3 films. Journal of Applied Physics, 2016, 119, .	1.1	19
77	Effect of atomic layer deposition temperature on current conduction in Al2O3 films formed using H2O oxidant. Journal of Applied Physics, 2016, 120, .	1.1	25
78	High voltage breakdown (1.8 kV) of hydrogenated black diamond field effect transistor. Applied Physics Letters, 2016, 109, .	1.5	30
79	Hydrogen-terminated diamond vertical-type metal oxide semiconductor field-effect transistors with a trench gate. Applied Physics Letters, 2016, 109, .	1.5	38
80	Contact Conductivity of Uncapped Carbon Nanotubes Formed by Silicon Carbide Decomposition. Journal of Physical Chemistry C, 2016, 120, 6232-6238.	1.5	4
81	Polycrystalline boron-doped diamond with an oxygen-terminated surface channel as an electrolyte-solution-gate field-effect transistor for pH sensing. Electrochimica Acta, 2016, 212, 10-15.	2.6	15
82	Spin-induced anomalous magnetoresistance at the (100) surface of hydrogen-terminated diamond. Physical Review B, 2016, 94, .	1.1	12
83	Radially oriented nanostrand electrodes to boost glucose sensing in mammalian blood. Biosensors and Bioelectronics, 2016, 77, 656-665.	5.3	41
84	Research Progress on Materials for MEMS and Electronics Devices of Electronics Materials Development Group. Materia Japan, 2015, 54, 232-235.	0.1	0
85	Oneâ€Pot Fabrication of Dendritic NiO@carbon–nitrogen Dot Electrodes for Screening Blood Glucose Level in Diabetes. Advanced Healthcare Materials, 2015, 4, 2110-2119.	3.9	52
86	Functionalized carbon microarrays platform for high sensitive detection of HIV-Tat peptide. RSC Advances, 2015, 5, 65042-65047.	1.7	5
87	Direct partial CH3 termination into carboxyl terminated diamond surface for biosensor. , 2015, , .		Ο
88	Signature of high <i>T</i> c above 25 K in high quality superconducting diamond. Applied Physics Letters, 2015, 106, 052601.	1.5	54
89	Very low Schottky barrier height at carbon nanotube and silicon carbide interface. Applied Physics Letters, 2015, 106, .	1.5	13
90	lsotope analysis of diamond-surface passivation effect of high-temperature H2O-grown atomic layer deposition-Al2O3 films. Journal of Applied Physics, 2015, 117, .	1.1	29

#	Article	IF	CITATIONS
91	Blocking characteristics of diamond junctions with a punch-through design. Journal of Applied Physics, 2015, 117, 124503.	1.1	18
92	Electron transport dependence of nanoscale hemeprotein molecular structures for engineering electrochemical nanosensor. Nano Structures Nano Objects, 2015, 2, 35-44.	1.9	5
93	Room-temperature amorphous alloy field-effect transistor exhibiting particle and wave electronic transport. Journal of Applied Physics, 2015, 117, 084302.	1.1	1
94	Large-current-controllable carbon nanotube field-effect transistor in electrolyte solution. Applied Physics Letters, 2015, 106, .	1.5	4
95	Repulsive effects of hydrophobic diamond thin films on biomolecule detection. Applied Surface Science, 2015, 328, 314-318.	3.1	6
96	Quantum oscillations of the two-dimensional hole gas at atomically flat diamond surfaces. Physical Review B, 2014, 89, .	1.1	28
97	Substitution Effects of Cr or Fe on the Curie Temperature for Mn-Based Layered Compounds MnAlGe and MnGaGe With Cu ₂ Sb-Type Structure. IEEE Transactions on Magnetics, 2014, 50, 1-4.	1.2	13
98	High-reliability passivation of hydrogen-terminated diamond surface by atomic layer deposition of Al2O3. Journal of Applied Physics, 2014, 115, .	1.1	70
99	C-H surface diamond field effect transistors for high temperature (400 °C) and high voltage (500 V) operation. Applied Physics Letters, 2014, 105, .	1.5	161
100	Diamond surface conductivity: Properties, devices, and sensors. MRS Bulletin, 2014, 39, 542-548.	1.7	64
101	Comparison of Different Oxidation Techniques for Biofunctionalization of Pyrolyzed Carbon. Material Science Research India, 2014, 11, 01-08.	0.9	8
102	Figure of merit of diamond power devices based on accurately estimated impact ionization processes. Journal of Applied Physics, 2013, 114, .	1.1	49
103	Effect of hydrogen and cluster morphology on the electronic behavior of Ni-Nb-Zr-H glassy alloys with subnanometer-sized icosahedral Zr5Ni5Nb5 clusters. European Physical Journal D, 2013, 67, 1.	0.6	2
104	Understanding the stability of a sputtered Al buffer layer for single-walled carbon nanotube forest synthesis. Carbon, 2013, 57, 401-409.	5.4	13
105	Increasing the length of a single-wall carbon nanotube forest by adding titanium to a catalytic substrate. Carbon, 2013, 57, 79-87.	5.4	14
106	SPATIAL VARIATION OF TUNNELING SPECTRA IN (111)-ORIENTED FILMS OF BORON-DOPED DIAMOND PROBED BY STM/STS. International Journal of Modern Physics B, 2013, 27, 1362014.	1.0	4
107	Platelet-derived growth factor oncoprotein detection using three-dimensional carbon microarrays. Biosensors and Bioelectronics, 2013, 39, 118-123.	5.3	30
108	Effects of diamond-FET-based RNA aptamer sensing for detection of real sample of HIV-1 Tat protein. Biosensors and Bioelectronics, 2013, 40, 277-282.	5.3	83

#	Article	IF	CITATIONS
109	Low-Temperature Transport Properties of Holes Introduced by Ionic Liquid Gating in Hydrogen-Terminated Diamond Surfaces. Journal of the Physical Society of Japan, 2013, 82, 074718.	0.7	30
110	Accuracy assessment of sheet-charge approximation for Fowler-Nordheim tunneling into charged insulators. Journal of Applied Physics, 2013, 114, .	1.1	10
111	Effect of Hydrogen Absorption on Electrical Transport Properties for Ni ₃₆ Nb ₂₄ Zr ₄₀ Amorphous Alloy Ribbons. Materials Transactions, 2013, 54, 1339-1342.	0.4	4
112	High-Current Metal Oxide Semiconductor Field-Effect Transistors on H-Terminated Diamond Surfaces and Their High-Frequency Operation. Japanese Journal of Applied Physics, 2012, 51, 090111.	0.8	53
113	Fluorescence-Signaling Aptasensor for ATP and PDGF Detection on Functionalized Diamond Surface. Journal of the Electrochemical Society, 2012, 159, J182-J187.	1.3	11
114	Capacitance Distribution of Ni-Nb-Zr-H Glassy Alloys. Journal of Nanoscience and Nanotechnology, 2012, 12, 3848-3852.	0.9	5
115	High Priority of Nanocrystalline Diamond as a Biosensing Platform. Japanese Journal of Applied Physics, 2012, 51, 090125.	0.8	3
116	Refractory two-dimensional hole gas on hydrogenated diamond surface. Journal of Applied Physics, 2012, 112, .	1.1	54
117	Fabrication of carbon nanostructures using photo-nanoimprint lithography and pyrolysis. Journal of Micromechanics and Microengineering, 2012, 22, 045024.	1.5	34
118	Highly sensitive detection of platelet-derived growth factor on a functionalized diamond surface using aptamer sandwich design. Analyst, The, 2012, 137, 1692.	1.7	47
119	Controllable oxidization of boron doped nanodiamond covered with different solution via UV/ozone treatment. Diamond and Related Materials, 2012, 24, 146-152.	1.8	14
120	Effective Surface Functionalization of Nanocrystalline Diamond Films by Direct Carboxylation for PDGF Detection via Aptasensor. ACS Applied Materials & Interfaces, 2012, 4, 3526-3534.	4.0	31
121	Mesoporous NiO nanomagnets as catalysts and separators of chemical agents. Applied Catalysis B: Environmental, 2012, 127, 1-10.	10.8	48
122	Growth and electrical characterisation of δ-doped boron layers on (111) diamond surfaces. Journal of Applied Physics, 2012, 111, 033710.	1.1	37
123	Three-dimensional graphene nanosheet encrusted carbon micropillar arrays for electrochemical sensing. Nanoscale, 2012, 4, 3673.	2.8	52
124	Vertical SNS weak-link Josephson junction fabricated from only boron-doped diamond. Physical Review B, 2012, 85, .	1.1	14
125	High quality single-walled carbon nanotube synthesis using remote plasma CVD. Diamond and Related Materials, 2012, 24, 184-187.	1.8	18
126	Multidirectional porous NiO nanoplatelet-like mosaics as catalysts for green chemical transformations. Applied Catalysis B: Environmental, 2012, 123-124, 162-173.	10.8	35

#	Article	IF	CITATIONS
127	Boron δ-doped (111) diamond solution gate field effect transistors. Biosensors and Bioelectronics, 2012, 33, 152-157.	5.3	14
128	High-Current Metal Oxide Semiconductor Field-Effect Transistors on H-Terminated Diamond Surfaces and Their High-Frequency Operation. Japanese Journal of Applied Physics, 2012, 51, 090111.	0.8	40
129	High Priority of Nanocrystalline Diamond as a Biosensing Platform. Japanese Journal of Applied Physics, 2012, 51, 090125.	0.8	3
130	Higher coverage of carboxylic acid groups on oxidized single crystal diamond (001). Diamond and Related Materials, 2011, 20, 1319-1324.	1.8	43
131	Fabrication of Metal–Oxide–Diamond Field-Effect Transistors with Submicron-Sized Gate Length on Boron-Doped (111) H-Terminated Surfaces Using Electron Beam Evaporated SiO2 and Al2O3. Journal of Electronic Materials, 2011, 40, 247-252.	1.0	29
132	Diamond electrolyte solution gate FETs for DNA and protein sensors using DNA/RNA aptamers. Physica Status Solidi (A) Applications and Materials Science, 2011, 208, 2005-2016.	0.8	54
133	Photoemission study of electronic structure evolution across the metal–insulator transition of heavily B-doped diamond. Journal of Physics and Chemistry of Solids, 2011, 72, 582-584.	1.9	7
134	Human immunodeficiency virus trans-activator of transcription peptide detection via ribonucleic acid aptamer on aminated diamond biosensor. Applied Physics Letters, 2011, 99, .	1.5	10
135	Aptasensor for Oncoprotein Platelet-Derived Growth Factor Detection on Functionalized Diamond Surface by Signal-Off Optical Method. Applied Physics Express, 2011, 4, 027001.	1.1	10
136	Pressure effect of superconducting transition temperature for boron-doped (111) diamond films. Journal of Physics: Conference Series, 2010, 215, 012143.	0.3	3
137	Schottky barrier heights, carrier density, and negative electron affinity of hydrogen-terminated diamond. Physical Review B, 2010, 81, .	1.1	42
138	Superconductor-to-insulator transition in boron-doped diamond films grown using chemical vapor deposition. Physical Review B, 2010, 82, .	1.1	66
139	Critical concentrations of superconductor to insulator transition in (1 1 1) and (0 0 1) CVD boron-doped diamond. Physica C: Superconductivity and Its Applications, 2010, 470, S604-S607.	0.6	2
140	Ultrashallow TiC Source/Drain Contacts in Diamond MOSFETs Formed by Hydrogenation-Last Approach. IEEE Transactions on Electron Devices, 2010, 57, 966-972.	1.6	42
141	Fabrication of calcium ion sensitive diamond field effect transistors (FETs) based on immobilized calmodulin. Materials Letters, 2010, 64, 2321-2324.	1.3	2
142	Stacked SNS Josephson junction of all boron doped diamond. Physica C: Superconductivity and Its Applications, 2010, 470, S613-S615.	0.6	11
143	Cross-sectional TEM study and film thickness dependence of Tc in heavily boron-doped superconducting diamond. Physica C: Superconductivity and Its Applications, 2010, 470, S610-S612.	0.6	16
144	Electronic structures of B 2p levels in homo-epitaxial growth boron-doped diamond by soft X-rays absorption spectroscopy. Physica C: Superconductivity and Its Applications, 2010, 470, S671-S672.	0.6	2

#	Article	IF	CITATIONS
145	Aptamer-based biosensor for sensitive PDGF detection using diamond transistor. Biosensors and Bioelectronics, 2010, 26, 1599-1604.	5.3	29
146	Low-temperature synthesis of multiwalled carbon nanotubes by graphite antenna CVD in a hydrogen-free atmosphere. Carbon, 2010, 48, 825-831.	5.4	13
147	High-Performance P-Channel Diamond Metal–Oxide–Semiconductor Field-Effect Transistors on H-Terminated (111) Surface. Applied Physics Express, 2010, 3, 044001.	1.1	62
148	Low drift and small hysteresis characteristics of diamond electrolyte-solution-gate FET. Journal Physics D: Applied Physics, 2010, 43, 374020.	1.3	25
149	Ishizaka <i>etÂal.</i> Reply:. Physical Review Letters, 2009, 102, .	2.9	0
150	Direct amination on 3-dimensional pyrolyzed carbon micropattern surface for DNA detection. Materials Letters, 2009, 63, 2680-2683.	1.3	28
151	Mathematical study of trade-off relations in logistics systems. Journal of Computational and Applied Mathematics, 2009, 232, 122-126.	1.1	3
152	Soft X-ray Core-Level Photoemission Study of Boron Sites in Heavily Boron-Doped Diamond Films. Journal of the Physical Society of Japan, 2009, 78, 034703.	0.7	3
153	Low-temperature STM/STS studies on boron-doped (111) diamond films. Journal of Physics and Chemistry of Solids, 2008, 69, 3027-3030.	1.9	7
154	Functionalization of ultradispersed diamond for DNA detection. Journal of Nanoparticle Research, 2008, 10, 69-75.	0.8	19
155	Pressure effect of superconducting transition temperature for boron-doped diamond films. Physica C: Superconductivity and Its Applications, 2008, 468, 1228-1230.	0.6	5
156	Near EF electronic structure of heavily boron-doped superconducting diamond. Journal of Physics and Chemistry of Solids, 2008, 69, 2978-2981.	1.9	9
157	Highly selective growth of vertically aligned doubleâ€walled carbon nanotubes by a controlled heating method and their electric doubleâ€layer capacitor properties. Physica Status Solidi - Rapid Research Letters, 2008, 2, 53-55.	1.2	13
158	Detection of Mismatched DNA on Partially Negatively Charged Diamond Surfaces by Optical and Potentiometric Methods. Journal of the American Chemical Society, 2008, 130, 13251-13263.	6.6	62
159	Holes in the Valence Band of Superconducting Boron-Doped Diamond Film Studied by Soft X-ray Absorption and Emission Spectroscopy. Journal of the Physical Society of Japan, 2008, 77, 054711.	0.7	22
160	Channel mobility evaluation for diamond MOSFETs using gate-to-channel capacitance measurement. Diamond and Related Materials, 2008, 17, 1256-1258.	1.8	7
161	Vertically aligned carbon nanotube growth from Ni nanoparticles prepared by ion implantation. Diamond and Related Materials, 2008, 17, 1443-1446.	1.8	3
162	Characterization of boron-doped diamonds using 11B high-resolution NMR at high magnetic fields. Diamond and Related Materials, 2008, 17, 1835-1839.	1.8	6

#	Article	IF	CITATIONS
163	Robustness of CNT Via Interconnect Fabricated by Low Temperature Process over a High-Density Current. , 2008, , .		24
164	Mechanism Analysis of Interrupted Growth of Single-Walled Carbon Nanotube Arrays. Nano Letters, 2008, 8, 886-890.	4.5	43
165	Precise detection of singly mismatched DNA with functionalized diamond electrolyte solution gate FET , 2008, , .		1
166	DC and RF Performance of Diamond MISFETs with Alumina Gate Insulator. Materials Science Forum, 2008, 600-603, 1349-1351.	0.3	2
167	Enhanced field emission properties of vertically aligned double-walled carbon nanotube arrays. Nanotechnology, 2008, 19, 415703.	1.3	54
168	Temperature-Dependent Localized Excitations of Doped Carriers in Superconducting Diamond. Physical Review Letters, 2008, 100, 166402.	2.9	25
169	Spontaneous polarization model for surface orientation dependence of diamond hole accumulation layer and its transistor performance. Applied Physics Letters, 2008, 92, .	1.5	106
170	Electrical Properties of Carbon Nanotubes Grown at a Low Temperature for Use as Interconnects. Japanese Journal of Applied Physics, 2008, 47, 1985.	0.8	73
171	p-type Surface Accumulation Layer of Hydrogen Terminated Diamond. Hyomen Kagaku, 2008, 29, 144-150.	0.0	2
172	11B Nuclear Magnetic Resonance Study on Existence of Boron–Hydrogen Complex in Boron-Doped Diamond. Japanese Journal of Applied Physics, 2007, 46, L1138-L1140.	0.8	7
173	Core-level electronic structure evolution of heavily boron-doped superconducting diamond studied with hard x-ray photoemission spectroscopy. Physical Review B, 2007, 75, .	1.1	20
174	Observation of a Superconducting Gap in Boron-Doped Diamond by Laser-Excited Photoemission Spectroscopy. Physical Review Letters, 2007, 98, 047003.	2.9	40
175	Miniaturized diamond field-effect transistors for application in biosensors in electrolyte solution. Applied Physics Letters, 2007, 90, 063901.	1.5	24
176	High-performance p-channel diamond MOSFETs with alumina gate insulator. , 2007, , .		45
177	Electronic Devices. , 2007, , 231-280.		1
178	Phonon softening in superconducting diamond. Physical Review B, 2007, 75, .	1.1	40
179	Growth Kinetics of 0.5 cm Vertically Aligned Single-Walled Carbon Nanotubes. Journal of Physical Chemistry B, 2007, 111, 1907-1910.	1.2	165
180	Low temperature grown carbon nanotube interconnects using inner shells by chemical mechanical polishing. Applied Physics Letters, 2007, 91, .	1.5	100

#	Article	IF	CITATIONS
181	Microscopic evidence for evolution of superconductivity by effective carrier doping in boron-doped diamond:B11â^`NMRstudy. Physical Review B, 2007, 75, .	1.1	36
182	Diamond MISFETs fabricated on high quality polycrystalline CVD diamond. , 2007, , .		1
183	Superconducting properties of homoepitaxial CVD diamond. Diamond and Related Materials, 2007, 16, 911-914.	1.8	104
184	Growth of dense single-walled carbon nanotubes in nano-sized silicon dioxide holes for future microelectronics. Carbon, 2007, 45, 2351-2355.	5.4	15
185	Energy gap and surface structure of superconducting diamond films probed by scanning tunneling microscopy. Physica C: Superconductivity and Its Applications, 2007, 460-462, 210-211.	0.6	4
186	Low-Energy Electrodynamics of Superconducting Diamond. Physical Review Letters, 2006, 97, 097002.	2.9	55
187	Electronic Structures of Heavily Boron-doped Superconducting Diamond Films. Materials Research Society Symposia Proceedings, 2006, 956, 1.	0.1	Ο
188	Enhancement of field emission characteristics of tungsten emitters by single-walled carbon nanotube modification. Applied Physics Letters, 2006, 88, 033116.	1.5	24
189	DNA Micropatterning on Polycrystalline Diamond via One-Step Direct Amination. Langmuir, 2006, 22, 3728-3734.	1.6	111
190	Label-free DNA sensors using ultrasensitive diamond field-effect transistors in solution. Physical Review E, 2006, 74, 041919.	0.8	93
191	Characterization of DNA Hybridization on Partially Aminated Diamond by Aromatic Compounds. Langmuir, 2006, 22, 11245-11250.	1.6	47
192	Semi-quantitative study on the fabrication of densely packed and vertically aligned single-walled carbon nanotubes. Carbon, 2006, 44, 2009-2014.	5.4	84
193	pH-sensitive diamond field-effect transistors (FETs) with directly aminated channel surface. Analytica Chimica Acta, 2006, 573-574, 3-8.	2.6	39
194	Laser-excited photoemission spectroscopy study of superconducting boron-doped diamond. Science and Technology of Advanced Materials, 2006, 7, S17-S21.	2.8	14
195	Acoustic and optical phonons in metallic diamond. Science and Technology of Advanced Materials, 2006, 7, S31-S36.	2.8	11
196	Superconductivity and low temperature electrical transport in B-doped CVD nanocrystalline diamond. Science and Technology of Advanced Materials, 2006, 7, S41-S44.	2.8	14
197	Scanning tunneling microscopy and spectroscopy studies of superconducting boron-doped diamond films. Science and Technology of Advanced Materials, 2006, 7, S22-S26.	2.8	15
198	Stereophotographs of diamond and graphite. Science and Technology of Advanced Materials, 2006, 7, 45-48.	2.8	12

#	Article	IF	CITATIONS
199	Characterization of Direct Immobilized Probe DNA on Partially Functionalized Diamond Solution-Gate Field-Effect Transistors. Japanese Journal of Applied Physics, 2006, 45, L1114-L1117.	0.8	18
200	Fabrication of T-Shaped Gate Diamond Metal–Insulator–Semiconductor Field-Effect Transistors. Japanese Journal of Applied Physics, 2006, 45, 5681-5684.	0.8	9
201	Direct immobilization of DNA on partially functionalized diamond surface. Materials Research Society Symposia Proceedings, 2006, 950, 1.	0.1	Ο
202	Characterization of diamond metal-insulator-semiconductor field-effect transistors with aluminum oxide gate insulator. Applied Physics Letters, 2006, 88, 112117.	1.5	35
203	Trapping mechanism on oxygen-terminated diamond surfaces. Applied Physics Letters, 2006, 89, 203503.	1.5	27
204	Evaluations of Electrical Properties for ZnTe Thin Films Electrodeposited from a Citric Acid Bath with a Hall Effect Measurement. Nippon Kinzoku Gakkaishi/Journal of the Japan Institute of Metals, 2005, 69, 298-302.	0.2	0
205	Characterization of locally modified diamond surface using Kelvin probe force microscope. Surface Science, 2005, 581, 207-212.	0.8	58
206	Origin of the metallic properties of heavily boron-doped superconducting diamond. Nature, 2005, 438, 647-650.	13.7	244
207	Very High Yield Growth of Vertically Aligned Single-Walled Carbon Nanotubes by Point-Arc Microwave Plasma CVD. Chemical Vapor Deposition, 2005, 11, 127-130.	1.4	85
208	Distribution Theoretic Approach to Multi-phase Flow. Mathematics in Industry, 2005, , 217-231.	0.1	0
209	RF Diamond Transistors: Current Status and Future Prospects. Japanese Journal of Applied Physics, 2005, 44, 7789-7794.	0.8	21
210	Micropatterning Oligonucleotides on Single-Crystal Diamond Surface by Photolithography. Japanese Journal of Applied Physics, 2005, 44, L295-L298.	0.8	8
211	Electrical Properties of Diamond MISFETs with Submicron-Sized Gate on Boron-Doped (111) Surface. Materials Research Society Symposia Proceedings, 2005, 891, 1.	0.1	Ο
212	Superconductivity in polycrystalline diamond thin films. Diamond and Related Materials, 2005, 14, 1936-1938.	1.8	72
213	Fabrication of diamond MISFET with micron-sized gate length on boron-doped (111) surface. Diamond and Related Materials, 2005, 14, 2043-2046.	1.8	11
214	An electron-spectroscopic view of CVD diamond surface conductivity. Diamond and Related Materials, 2005, 14, 459-465.	1.8	12
215	Low Temperature Synthesis of Extremely Dense and Vertically Aligned Single-Walled Carbon Nanotubes. Japanese Journal of Applied Physics, 2005, 44, 1558-1561.	0.8	130
216	Direct Evidence for Root Growth of Vertically Aligned Single-Walled Carbon Nanotubes by Microwave Plasma Chemical Vapor Deposition. Journal of Physical Chemistry B, 2005, 109, 19556-19559.	1.2	68

#	Article	IF	CITATIONS
217	Memory effect of diamond in-plane-gated field-effect transistors. Applied Physics Letters, 2004, 85, 139-141.	1.5	10
218	Surface-modified Diamond Field-effect Transistors for Enzyme-immobilized Biosensors. Japanese Journal of Applied Physics, 2004, 43, L814-L817.	0.8	51
219	Large-Area Synthesis of Carbon Nanofibers by Low-Power Microwave Plasma-Assisted CVD. Chemical Vapor Deposition, 2004, 10, 125-128.	1.4	21
220	Synthesis of highly oriented and dense conical carbon nanofibers by a DC bias-enhanced microwave plasma CVD method. Thin Solid Films, 2004, 464-465, 315-318.	0.8	12
221	Selective growth of carbon nanostructures on nickel implanted nanopyramid array. Applied Surface Science, 2004, 234, 72-77.	3.1	9
222	Over 20-GHz Cutoff Frequency Submicrometer-Gate Diamond MISFETs. IEEE Electron Device Letters, 2004, 25, 480-482.	2.2	56
223	Superconductivity in diamond thin films well above liquid helium temperature. Applied Physics Letters, 2004, 85, 2851-2853.	1.5	277
224	Chapter 7 Diamond held effect transistors using h-terminated surfaces. Semiconductors and Semimetals, 2004, , 311-338.	0.4	2
225	Electron-spectroscopy and -diffraction study of the conductivity of CVD diamond ()2×1 surface. Surface Science, 2003, 529, 180-188.	0.8	9
226	Clâ^' sensitive biosensor used electrolyte-solution-gate diamond FETs. Biosensors and Bioelectronics, 2003, 19, 137-140.	5.3	44
227	Diamond nanofabrication and characterization for biosensing application. Physica Status Solidi A, 2003, 199, 39-43.	1.7	28
228	Ozone-treated channel diamond field-effect transistors. Diamond and Related Materials, 2003, 12, 1971-1975.	1.8	55
229	High performance diamond MISFETs using CaF2 gate insulator. Diamond and Related Materials, 2003, 12, 399-402.	1.8	29
230	Effect of iodide ions on the hydrogen-terminated and partially oxygen-terminated diamond surface. Diamond and Related Materials, 2003, 12, 618-622.	1.8	35
231	Deep sub-micron gate diamond MISFETs. Diamond and Related Materials, 2003, 12, 1814-1818.	1.8	11
232	Initial growth of heteroepitaxial diamond on Ir (001)/MgO (001) substrates using antenna-edge-type microwave plasma assisted chemical vapor deposition. Diamond and Related Materials, 2003, 12, 246-250.	1.8	27
233	Non-linear increases in excitonic emission in synthetic type-lla diamond. Diamond and Related Materials, 2003, 12, 1995-1998.	1.8	5
234	Fabrication of diamond in-plane-gated field effect transistors using oxygen plasma etching. Diamond and Related Materials, 2003, 12, 408-412.	1.8	6

#	Article	IF	CITATIONS
235	Control wettability of the hydrogen-terminated diamond surface and the oxidized diamond surface using an atomic force microscope. Diamond and Related Materials, 2003, 12, 560-564.	1.8	85
236	Cryogenic operation of surface-channel diamond field-effect transistors. Diamond and Related Materials, 2003, 12, 1800-1803.	1.8	8
237	Cathodoluminescence and Hall-effect measurements in sulfur-doped chemical-vapor-deposited diamond. Applied Physics Letters, 2003, 82, 2074-2076.	1.5	26
238	Fabrication of single-hole transistors on hydrogenated diamond surface using atomic force microscope. Applied Physics Letters, 2002, 81, 2854-2856.	1.5	36
239	Effect of Cl-Ionic Solutions on Electrolyte-Solution-Gate Diamond Field-Effect Transistors. Japanese Journal of Applied Physics, 2002, 41, 2595-2597.	0.8	20
240	RF Performance of High Transconductance and High-Channel-Mobility Surface-Channel Polycrystalline Diamond Metal-Insulator-Semiconductor Field-Effect Transistors. Japanese Journal of Applied Physics, 2002, 41, 2611-2614.	0.8	24
241	Investigation of Current-Voltage Characteristics of Oxide Region Induced by Atomic Force Microscope on Hydrogen-Terminated Diamond Surface. Japanese Journal of Applied Physics, 2002, 41, 4980-4982.	0.8	10
242	Microwave Performance of Diamond Field-Effect Transistors. Japanese Journal of Applied Physics, 2002, 41, 2591-2594.	0.8	2
243	Nanoscale Modification of the Hydrogen-Terminated Diamond Surface Using Atomic Force Microscope. Japanese Journal of Applied Physics, 2002, 41, 4983-4986.	0.8	10
244	Low-temperature operation of diamond surface-channel field-effect transistors. Materials Research Society Symposia Proceedings, 2002, 719, 551.	0.1	0
245	RF performance of diamond MISFETs. IEEE Electron Device Letters, 2002, 23, 121-123.	2.2	22
246	Fabrication of heteroepitaxial diamond thin films on Ir(001)/MgO(001) substrates using antenna-edge-type microwave plasma-assisted chemical vapor deposition. Diamond and Related Materials, 2002, 11, 478-481.	1.8	10
247	Fabrication of diamond single-hole transistors using AFM anodization process. Diamond and Related Materials, 2002, 11, 387-391.	1.8	30
248	DC and RF characteristics of 0.7-μm-gate-length diamond metal–insulator–semiconductor field effect transistor. Diamond and Related Materials, 2002, 11, 378-381.	1.8	24
249	Heteroepitaxial diamond thin film growth on Ir(001)/MgO(001) substrate by antenna-edge plasma assisted chemical vapor deposition. Journal of Crystal Growth, 2002, 237-239, 1277-1280.	0.7	5
250	Potential applications of surface channel diamond field-effect transistors. Diamond and Related Materials, 2001, 10, 1743-1748.	1.8	33
251	Cathodoluminescence of phosphorus doped (111) homoepitaxial diamond thin films. Diamond and Related Materials, 2001, 10, 1652-1654.	1.8	28
252	High-frequency performance of diamond field-effect transistor. IEEE Electron Device Letters, 2001, 22, 390-392.	2.2	91

#	Article	IF	CITATIONS
253	Nanodevice fabrication on hydrogenated diamond surface using atomic force microscope. Materials Research Society Symposia Proceedings, 2001, 675, 1.	0.1	3
254	Fabrication of 0.1 µm channel diamond Metal-Insulator-Semiconductor Field-Effect Transistor. Materials Research Society Symposia Proceedings, 2001, 680, 1.	0.1	3
255	Electrolyte-Solution-Gate FETs Using Diamond Surface for Biocompatible Ion Sensors. Physica Status Solidi A, 2001, 185, 79-83.	1.7	122
256	High-Performance Surface-Channel Diamond Field-Effect Transistors. Materials Science Forum, 2001, 353-356, 815-0.	0.3	0
257	Diamond Deposition on a Large-Area Substrate by Plasma-Assisted Chemical Vapor Deposition Using an Antenna-Type Coaxial Microwave Plasma Generator. Japanese Journal of Applied Physics, 2001, 40, L698-L700.	0.8	16
258	Characterization of Diamond Surface-Channel Metal-Semiconductor Field-Effect Transistor with Device Simulation. Japanese Journal of Applied Physics, 2001, 40, 3101-3107.	0.8	16
259	Excitonic recombination radiation in phosphorus-doped CVD diamonds. Physical Review B, 2001, 64, .	1.1	21
260	Control of adsorbates and conduction on CVD-grown diamond surface, using scanning probe microscope. Applied Surface Science, 2000, 159-160, 578-582.	3.1	32
261	Cu/CaF2/Diamond Metal-Insulator-Semiconductor Field-Effect Transistor Utilizing Self-Aligned Gate Fabrication Process. Japanese Journal of Applied Physics, 2000, 39, L908-L910.	0.8	32
262	Nanofabrication on Hydrogen-Terminated Diamond Surfaces by Atomic Force Microscope Probe-Induced Oxidation. Japanese Journal of Applied Physics, 2000, 39, 4631-4632.	0.8	44
263	Surface Order Evaluation of the Heteroepitaxial Diamond Film Grown on an Inclined β-SiC(001). Japanese Journal of Applied Physics, 2000, 39, 4372-4373.	0.8	5
264	High-Performance Diamond Metal-Semiconductor Field-Effect Transistor with 1 µm Gate Length. Japanese Journal of Applied Physics, 1999, 38, L1222-L1224.	0.8	47
265	Surface p-channel metal-oxide-semiconductor field effect transistors fabricated on hydrogen terminated (001) surfaces of diamond. Solid-State Electronics, 1999, 43, 1465-1471.	0.8	20
266	Fundamental study of moving object tracking using local moments. Electronics and Communications in Japan, Part III: Fundamental Electronic Science (English Translation of Denshi Tsushin Gakkai) Tj ETQq0 0 0 rgBT	/ Qu erlock	1 0 Tf 50 21
267	High-preformance diamond surface-channel field-effect transistors and their operation mechanism. Diamond and Related Materials, 1999, 8, 927-933.	1.8	96
268	MOSFETs on polished surfaces of polycrystalline diamond. Diamond and Related Materials, 1999, 8, 1831-1833.	1.8	15
269	Application and device modeling of diamond FET using surface semiconductive layers. Electronics and Communications in Japan, 1998, 81, 19-27.	0.2	3
270	Surface morphology and surface p-channel field effect transistor on the heteroepitaxial diamond deposited on inclined β-SiC(001) surfaces. Applied Physics Letters, 1998, 72, 1878-1880.	1.5	18

#	Article	IF	CITATIONS
271	MESFETs and MOSFETs on Hydrogen-Terminated Diamond Surfaces. Materials Science Forum, 1998, 264-268, 977-980.	0.3	4
272	Enhancement/Depletion Surface Channel Field Effect Transistors of Diamond and Their Logic Circuits. Japanese Journal of Applied Physics, 1997, 36, 7133-7139.	0.8	25
273	Heteroepitaxial growth of highly oriented diamond on cubic silicon carbide. Journal of Applied Physics, 1997, 81, 3490-3493.	1.1	84
274	Surface characterization of smooth heteroepitaxial diamond layers on β-SiC (001). Diamond and Related Materials, 1997, 6, 277-281.	1.8	8
275	Comparative study of excitonic recombination radiation from diamonds grown by CVD and HP/HT methods. Diamond and Related Materials, 1997, 6, 1668-1673.	1.8	0
276	Enhancement/depletion MESFETs of diamond and their logic circuits. Diamond and Related Materials, 1997, 6, 339-343.	1.8	62
277	Device modeling of high performance diamond MESFETs using p-type surface semiconductive layers. Diamond and Related Materials, 1997, 6, 865-868.	1.8	15
278	Hydrogen-terminated diamond surfaces and interfaces. Surface Science Reports, 1996, 26, 205-206.	3.8	529
279	Electron Affinity and Surface Re-ordering of Homoepitaxial Diamond (100). Japanese Journal of Applied Physics, 1996, 35, 5444-5447.	0.8	5
280	Electrically Isolated Metal-Semiconductor Field Effect Transistors and Logic Circuits on Homoepitaxial Diamonds. Japanese Journal of Applied Physics, 1996, 35, L1165-L1168.	0.8	22
281	Scanning-tunneling-microscope observation of the homoepitaxial diamond (001) 2×1 reconstruction observed under atmospheric pressure. Physical Review B, 1995, 52, 11351-11358.	1.1	133
282	Heteroepitaxial growth of smooth and continuous diamond thin films on silicon substrates via high quality silicon carbide buffer layers. Applied Physics Letters, 1995, 66, 583-585.	1.5	105
283	Fabrication and Characterization of Metal-Semiconductor Field-Effect Transistor Utilizing Diamond Surface-Conductive Layer. Japanese Journal of Applied Physics, 1995, 34, 4677-4681.	0.8	36
284	Initial Growth of Heteroepitaxial Diamond on Si(001) Substrates via Î ² -SiC Buffer Layer. Japanese Journal of Applied Physics, 1995, 34, 4898-4904.	0.8	51
285	Heteroepitaxial Growth of Tungsten Carbide Films on W(110) by Plasma-Enhanced Chemical Vapor Deposition. Japanese Journal of Applied Physics, 1995, 34, 3628-3630.	0.8	11
286	Cathodoluminescence from highâ€pressure synthetic and chemicalâ€vaporâ€deposited diamond. Journal of Applied Physics, 1995, 77, 1729-1734.	1.1	66
287	Plasma-Enhanced Diamond Nucleation on Si. Japanese Journal of Applied Physics, 1994, 33, L194-L196.	0.8	32
288	Electric Properties of Metal/Diamond Interfaces Utilizing Hydrogen-Terminated Surfaces of Homoepitaxial Diamonds. Japanese Journal of Applied Physics, 1994, 33, L708-L711.	0.8	66

#	Article	IF	CITATIONS
289	Temperature and Incident Beam-Current Dependence of Dominant Free-Exciton Recombination Radiation from High-Purity Chemical Vapor Deposition (CVD) Diamonds. Japanese Journal of Applied Physics, 1994, 33, L1063-L1065.	0.8	8
290	Dominant freeâ€exciton recombination radiation in chemical vapor deposited diamonds. Applied Physics Letters, 1994, 64, 451-453.	1.5	41
291	Enhancement mode metalâ€semiconductor field effect transistors using homoepitaxial diamonds. Applied Physics Letters, 1994, 65, 1563-1565.	1.5	166
292	Characterization of hydrogen-terminated CVD diamond surfaces and their contact properties. Diamond and Related Materials, 1994, 3, 961-965.	1.8	72
293	Effect of Deuterium Anneal on SiO2/Si(100) Interface Traps and MOS Tunneling Current of Ultrathin SiO2 Films. , 1994, , 211-216.		1
294	Reflection electron microscope and scanning tunneling microscope observations of CVD diamond (001) surfaces. Diamond and Related Materials, 1993, 2, 1271-1276.	1.8	24
295	Excitonic recombination radiation as characterization of diamonds using cathodoluminescence. Diamond and Related Materials, 1993, 2, 100-105.	1.8	26
296	Low-Pressure Diamond Nucleation and Growth on Cu Substrate. Japanese Journal of Applied Physics, 1993, 32, L200-L203.	0.8	14
297	Structure of Chemical Vapor Deposited Diamond (111) Surfaces by Scanning Tunneling Microscopy. Japanese Journal of Applied Physics, 1993, 32, L1771-L1774.	0.8	31
298	Effect of Deuterium Anneal on SiO2/Si(100) Interface Traps and Electron Spin Resonance Signals of Ultrathin SiO2Films. Japanese Journal of Applied Physics, 1993, 32, L569-L571.	0.8	8
299	Excitonic recombination radiation in undoped and boron-doped chemical-vapor-deposited diamonds. Physical Review B, 1993, 47, 3633-3637.	1.1	105
300	Persistent hole burning of the nitrogen vacancy center and the 2.16 eV center of chemicalâ€vapor deposited diamond. Applied Physics Letters, 1992, 61, 2138-2140.	1.5	8
301	Formation of optical centers in CVD diamond by electron and neutron irradiation. Diamond and Related Materials, 1992, 1, 470-477.	1.8	29
302	Low temperature diamond film fabrication using magneto-active plasma CVD. Diamond and Related Materials, 1992, 1, 168-174.	1.8	32
303	Properties of metal/diamond interfaces and effects of oxygen adsorbed onto diamond surface. Applied Physics Letters, 1991, 58, 940-941.	1.5	139
304	Large area diamond selective nucleation based epitaxy. Thin Solid Films, 1991, 206, 192-197.	0.8	10
305	Fabrication of diamond films under high density helium plasma formed by electron cyclotron resonance. Surface and Coatings Technology, 1991, 49, 374-380.	2.2	7
306	Effects of Plasma Potential on Diamond Deposition at Low Pressure Using Magneto-Microwave Plasma Chemical Vapor Deposition. Japanese Journal of Applied Physics, 1991, 30, 1279-1280.	0.8	9

#	Article	IF	CITATIONS
307	Fabrication of diamond films under high density helium plasma formed by electron cyclotron resonance. , 1991, , 374-380.		0
308	<title>Cathodoluminescence of exciton recombinations and vibronic color centers in undoped, boron-doped, and nitrogen-doped CVD diamonds</title> . , 1990, , .		2
309	<title>Observing diamond defects with an analytical color-fluorescence electron
microscope</title> . , 1990, , .		3
310	<title>Low-pressure CVD for wide-area diamond film deposition at low temperatures</title> . , 1990, , .		1
311	Nucleation control and selective growth of diamond particles formed with plasma CVD. Journal of Crystal Growth, 1990, 99, 1206-1210.	0.7	23
312	Interfacial structures and selective growth of diamond particles formed by plasma-assisted CVD. Applied Surface Science, 1990, 41-42, 572-579.	3.1	10
313	Preparation and characterization of wide area, high quality diamond film using magnetoactive plasma chemical vapour deposition. Surface and Coatings Technology, 1990, 43-44, 10-21.	2.2	26
314	Growth of diamond films at low pressure using magneto-microwave plasma CVD. Journal of Crystal Growth, 1990, 99, 1201-1205.	0.7	61
315	Cathodoluminescence imaging of semiconducting diamond formed by plasma CVD. Journal of Crystal Growth, 1990, 103, 65-70.	0.7	9
316	Luminescence and semiconducting properties of plasma CVD diamond. Vacuum, 1990, 41, 885-888.	1.6	5
317	Low-Temperature Synthesis of Diamond Films Using Magneto-Microwave Plasma CVD. Japanese Journal of Applied Physics, 1990, 29, L1483-L1485.	0.8	28
318	Effect of Electron and Neutron Irradiation on the Cathodoluminescence of Nitrogen-Doped CVD Diamond. Japanese Journal of Applied Physics, 1990, 29, L2232-L2235.	0.8	10
319	Cathodoluminescence and electroluminescence of undoped and boronâ€doped diamond formed by plasma chemical vapor deposition. Journal of Applied Physics, 1990, 67, 983-989.	1.1	100
320	Intrinsic and extrinsic recombination radiation from undoped and boronâ€doped diamonds formed by plasma chemical vapor deposition. Applied Physics Letters, 1990, 57, 1889-1891.	1.5	43
321	PREPARATION AND CHARACTERIZATION OF WIDE AREA, HIGH QUALITY DIAMOND FILM USING MAGNETOACTIVE PLASMA CHEMICAL VAPOUR DEPOSITION. , 1990, , 10-21.		1
322	The Synthesis of Diamond Films at Lower Pressure and Lower Temperature Using Magneto-Microwave Plasma CVD. Japanese Journal of Applied Physics, 1989, 28, L281-L283.	0.8	60
323	Deposition of wide-area diamond films in magneto-microwave plasma. Nuclear Instruments & Methods in Physics Research B, 1989, 37-38, 799-806.	0.6	13
324	Crystallinity and strength of diamond bombarded with low energy ion beams. Nuclear Instruments & Methods in Physics Research B, 1989, 39, 689-691.	0.6	5

#	Article	IF	CITATIONS
325	Selective nucleation and growth of diamond particles by plasmaâ€assisted chemical vapor deposition. Applied Physics Letters, 1989, 55, 1071-1073.	1.5	87
326	Properties of CVD Diamond/Metal Interface. Materials Research Society Symposia Proceedings, 1989, 162, 353.	0.1	11
327	Blue and Green Cathodoluminescence of Synthesized Diamond Films Formed by Plasma-Assisted Chemical Vapour Deposition. Japanese Journal of Applied Physics, 1988, 27, L683-L686.	0.8	67
328	Characterization of roughness and defects at an Si/SiO2interface formed by lateral solid phase epitaxy using highâ€resolution electron microscopy. Journal of Applied Physics, 1988, 63, 2641-2644.	1.1	3
329	Characterization of Diamond Particles and Films Formed by Plasma-Assisted Chemical Vapour Deposition Using High-Voltage Electron Microscopy. Japanese Journal of Applied Physics, 1987, 26, L1903-L1906.	0.8	25
330	Large Area Chemical Vapour Deposition of Diamond Particles and Films Using Magneto-Microwave Plasma. Japanese Journal of Applied Physics, 1987, 26, L1032-L1034.	0.8	122
331	Diamond-Like Carbon Thin Films. Tanso, 1987, 1987, 41-49.	0.1	2
332	High-Resolution Electron Microscope Study of Silicon on Insulator Structure Grown by Lateral Solid Phase Epitaxy. Japanese Journal of Applied Physics, 1986, 25, L814-L817.	0.8	7
333	Behavior of ionâ€implanted As atoms in Si during molybdenum disilicide formation. Journal of Applied Physics, 1986, 59, 3073-3076.	1.1	3
334	Numerical Solution of the Free Surface Drainage Problem of Two Immiscible Fluids by the Boundary-Element Method. Japanese Journal of Applied Physics, 1985, 24, 1359-1362.	0.8	6
335	Influence of Pt atoms on the low temperature formation of epitaxial Pd monosilicide. Journal of Applied Physics, 1985, 57, 244-248.	1.1	4
336	Structural Study of PtSi/(111)Si Interface with High-Resolution Electron Microscopy. Japanese Journal of Applied Physics, 1984, 23, L799-L802.	0.8	10
337	Reduction of contact resistivity by As redistribution during Pd2Si formation. Journal of Applied Physics, 1983, 54, 4679-4682.	1.1	15
338	On a Prognosis of Gear Surface Failure Using Sound of Gears. Bulletin of the JSME, 1982, 25, 834-841.	0.1	3
339	An application of the integrated penalty method to free boundary problems of laplace equation. Numerical Functional Analysis and Optimization, 1981, 3, 1-17.	0.6	13
340	Annealing behavior of spin density in UHV evaporated amorphous silicon. Physics Letters, Section A: General, Atomic and Solid State Physics, 1980, 78, 192-194.	0.9	5
341	High frequency application of high transconductance surface-channel diamond field-effect transistors. , 0, , .		1
342	Characterization of Hybridization on Diamond Solution-Gate Field-Effect Transistors for Detecting Single Mismatched Oligonucleotides. Applied Physics Express, 0, 1, 118001.	1.1	5